esa

ECOSPHERE

Modeling leaf area index in North America using a process-based terrestrial ecosystem model

YANG QU[1] AND QIANLAI ZHUANG[1,2,]†

[1]*Department of Earth, Atmospheric, and Planetary Sciences, Purdue University, 550 Stadium Mall Drive, West Lafayette, Indiana 47907 USA*
[2]*Department of Agronomy, Purdue University, 915 W. State Street, West Lafayette, Indiana 47907 USA*

Citation: Qu, Y., and Q. Zhuang. 2018. Modeling leaf area index in North America using a process-based terrestrial ecosystem model. Ecosphere 9(1):e02046. 10.1002/ecs2.2046

Abstract. Leaf area index (LAI) is often used to quantify plant production and evapotranspiration with terrestrial ecosystem models (TEMs). This study evaluated the LAI simulation in North America using a data assimilation technique and a process-based TEM as well as in situ and satellite data. We first optimized the parameters related to LAI in the TEM using a Markov Chain Monte Carlo method, and AmeriFlux site-level and regional LAI data from advanced very high-resolution radiometer. The parameterized model was then verified with the observed monthly LAI of major ecosystem types at site level. Simulated LAI was compared well with the observed data at sites of Harvard Forest (R^2 = 0.96), University of Michigan Biological Station (R^2 = 0.87), Howland Forest (R^2 = 0.96), Morgan Monroe State Forest (R^2 = 0.85), Shidler Tallgrass Prairie (R^2 = 0.82), and Donaldson (R^2 = 0.75). The root-mean-square error (RMSE) between modeled and satellite-based monthly LAI in North America is 1.4 m^2/m^2 for the period of 1985–2010. The simulated average monthly LAI in recent three decades increased by (3 ± 0.5)% in the region, with 1.24, 1.46, and 2.21 m^2/m^2 on average, in Alaska, Canada, and the conterminous United States, respectively, which is consistent with satellite data. The model performed well for wet tundra, boreal forest, temperate coniferous forests, temperate deciduous forests, grasslands, and xeric shrublands (RMSE < 1.5 m^2/m^2), but not for alpine tundra and xeric woodlands (RMSE > 1.5 m^2/m^2). Both the spring and fall LAI in the 2000s are higher than that in the 1980s in the region, suggesting that the leaf phenology has an earlier onset and later senescence in the 2000s. The average LAI increased in April and September by 0.03 and 0.24 m^2/m^2, respectively. This study provides a way to quantify LAI with ecosystem models, which will improve future carbon and water cycling studies.

Key words: leaf area index (LAI); model parameterization; phenology; terrestrial ecosystem model (TEM).

Received 24 July 2017; revised 6 October 2017; accepted 12 October 2017; final version received 12 November 2017. Corresponding Editor: Theresa M. Crimmins.

† **E-mail:** qzhuang@purdue.edu

INTRODUCTION

The interaction between biosphere and the atmosphere is strongly influenced by plant leaf phenology that refers to the temporal pattern of seasonal leaf onset and senescence (Arora and Boer 2005, Fisher et al. 2006). Under warming conditions, increasing greenhouse gas is expected to extend the growing season of plant leaf (Menzel and Fabian 1999, Beaubien and Freeland 2000, Chmielewski and Rötzer 2001). However, estimating leaf phenology with ecosystem models is still challenging although progress has been made in understanding the drivers of leaf phenology even at the molecular level (Sung and Amasino 2004). In the absence of process-based modeling of leaf phenology, empirical approaches in ecosystem and dynamic vegetation models have been tested with varying degrees of success (Linkosalo et al. 2008).

At regional scales, satellite-based vegetation indices have been used to characterize phenology (Asrar et al. 1989, Baret and Guyot 1991,

Zhang et al. 2003, Hurley et al. 2014, Jin and Eklundh 2014, Balzarolo et al. 2016). Previous studies focusing on phenology and vegetation indices have demonstrated that spatiotemporal data from remote sensing could be used to study phenological trends (Liang et al. 2014, Yue et al. 2015). Various vegetation indices are often computed using certain combinations of remote-sensing bands, such as red and infrared. For example, moderate-resolution imaging spectroradiometer (MODIS) provides a product of vegetation indices at a 16-d interval and a resolution of 500 m, from which we could identify the shift of green-up and senescence stages of different vegetation types.

Similar to other vegetation indices, leaf area index (LAI) is a good indicator of the seasonality of vegetation cover change (Beck et al. 2006), which can be used to characterize leaf phenology changes and is closely related to the global carbon and water cycles. Leaf area index is defined as total one-sided leaf area per unit ground surface area (Chen and Black 1992), which determines the amount of light intercepted by canopy (Chen and Cihlar 1996). It has been observed for various ecosystem types using LAI-2000, tracing radiation and architecture of canopies, and digital hemispherical photography in the field. Process-based models have also been used to estimate LAI directly or by combining remote-sensing data (e.g., Asrar et al. 1984, Asner et al. 2003). To date, there were still significant uncertainties in estimating LAI using ecosystem models (Richardson et al. 2012).

Here, we use a process-based ecosystem model, the terrestrial ecosystem model (TEM; Zhuang et al. 2003, 2010), to estimate LAI. We then use the simulated LAI to examine plant leaf phenology changes. Terrestrial ecosystem model is a process-based model that quantifies the dynamics of carbon, nitrogen, water, and energy at a monthly time step, using spatially explicit data of vegetation, climate, soil, and elevation (Raich et al. 1991, McGuire et al. 1992, Melillo et al. 1993, Zhuang et al. 2001, 2002, 2003, 2010, Felzer et al. 2004). Terrestrial ecosystem model consists of a set of ordinary differential equations that govern the exchanges of carbon and nitrogen between soils, vegetation, and the atmosphere. However, TEM's capability to simulate LAI has not yet been evaluated with observed data. Here, we take advantage of available site-level and satellite-based observation data to fully evaluate TEM. We then conduct LAI simulations for natural ecosystems in North America. The remote-sensing products for the entire region and various plant function types (PFTs) are used to evaluate the model. The changes in leaf phenology are then analyzed using LAI data for North America during the period of 1985–2010. This study focuses on improving quantification of LAI as an indicator of leaf phenology. We expect the correctly modeled LAI and leaf phenology will improve quantification of ecosystem water, energy, and carbon dynamics.

Methods

Overview

We first develop LAI algorithms in TEM. We then use a Markov Chain Monte Carlo (MCMC) method to acquire the best parameters at site and regional scales. Third, we verify site-level and regional LAI estimates using AmeriFlux observational data and the advanced very high-resolution radiometer (AVHRR) LAI product at a spatial resolution of 0.5° × 0.5°. Below, we first present our data organization at site and regional levels. Second, we describe the model development. Third, we describe the parameterization method and regional simulation protocols. Finally, we introduce how we conduct the leaf phenology change analysis by comparing model simulations and data product from remote sensing for North America from 1985 to 2010.

In situ and satellite data

Site-level LAI observational data are collected from AmeriFlux sites (Hagen et al. 2006, Urbanski et al. 2007, Sulman et al. 2009). Six sites including Harvard Forest, University of Michigan Biological Station, Howland Forest, Morgan Monroe State Forest, Shidler Tallgrass Prairie, and Donaldson are selected to cover major PFTs in this region (Figs. 1, 2). For site-level LAI calibration, we check all AmeriFlux sites that have LAI data and select the sites with continuous measurements for over 4 yr with measurements for every month. We use all the measurements available for our studying period in North America from these six sites to optimize LAI model parameters. These six sites are the only ones that meet our data selection criteria for our study in the region. We recognize

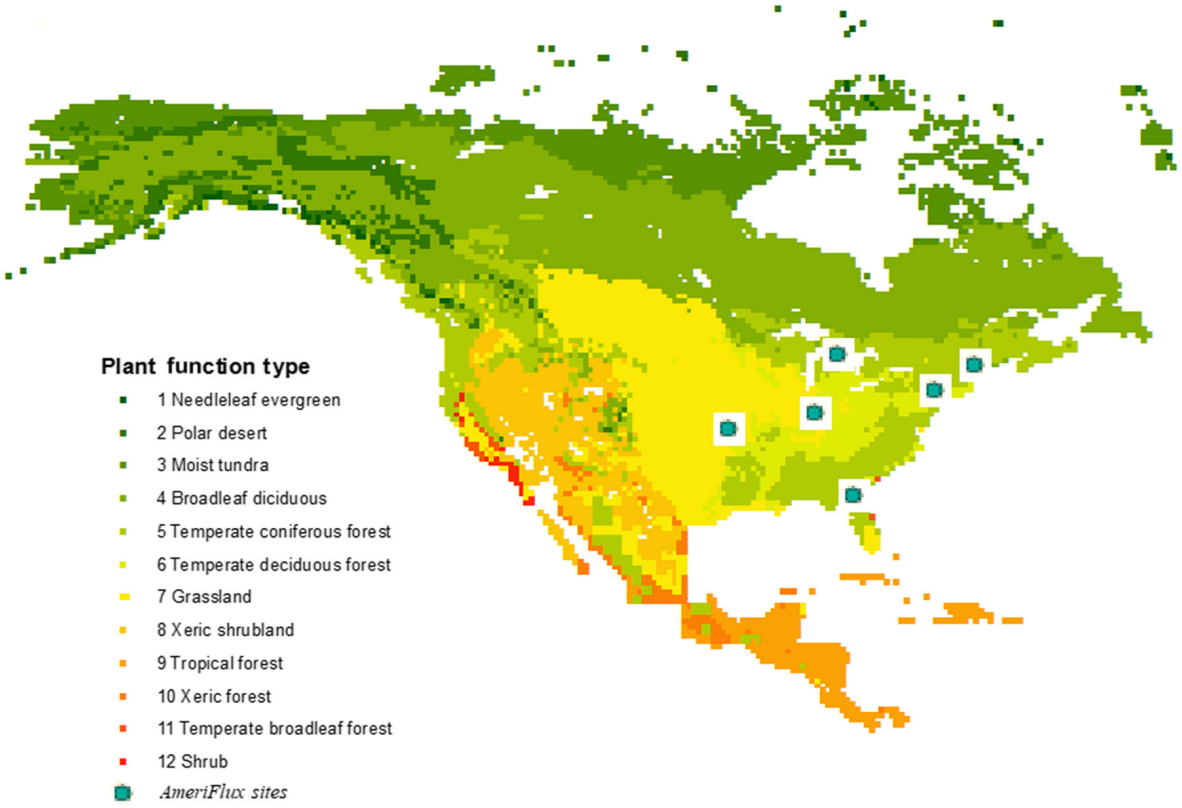

Fig. 1. Plant function type distribution in North America (Zhuang et al. 2003). AmeriFlux sites used for model calibration are also displayed.

these six sites represent a limited number of PFTs in North America. Thus, we further calibrate the model in a spatially explicit manner for regional LAI simulations to quantify regional LAI more accurately. The details of site and data description are documented in Table 1.

Two types of remote-sensing LAI products including AVHRR and global land surface satellite (GLASS) are used in this study. The third-generation LAI dataset from AVHRR (GIMMS LAI3 g) for the period from July 1985 to December 2010 is used (Myneni et al. 1997*a*, *b*). The AVHRR LAI product is produced using an artificial neural network method with resolution of 16 km and resampled to 0.5° × 0.5° degree (Anav et al. 2013, Claverie et al. 2016). The GLASS LAI algorithm (Liang et al. 2013) is based on time-series reflectance data using general regression neural networks. In general, the spatial patterns of GLASS LAI are consistent with MODIS and CYCLOPES products.

To conduct regional simulations, National Centers for Environmental Prediction monthly climate data in the period 1985–2010 at a spatial resolution 0.5° × 0.5° including precipitation, air temperature, and cloudiness are used. In addition, data of soil texture, elevation, and PFTs at the same spatial resolution are also used (Fig. 1; Zhuang et al. 2003). Advanced very high-resolution radiometer LAI product of 1985–2010 is used for regional model parameterization, while GLASS LAI is used for model evaluation.

Model description

In TEM, vegetation carbon (V_c) is modeled with a differential equation:

$$\frac{dVc}{dt} = \text{GPP} - R_A - L_C \quad (1)$$

where GPP refers to gross primary production, R_A refers to autotrophic respiration, and L_C refers to litterfall carbon. Gross primary production is

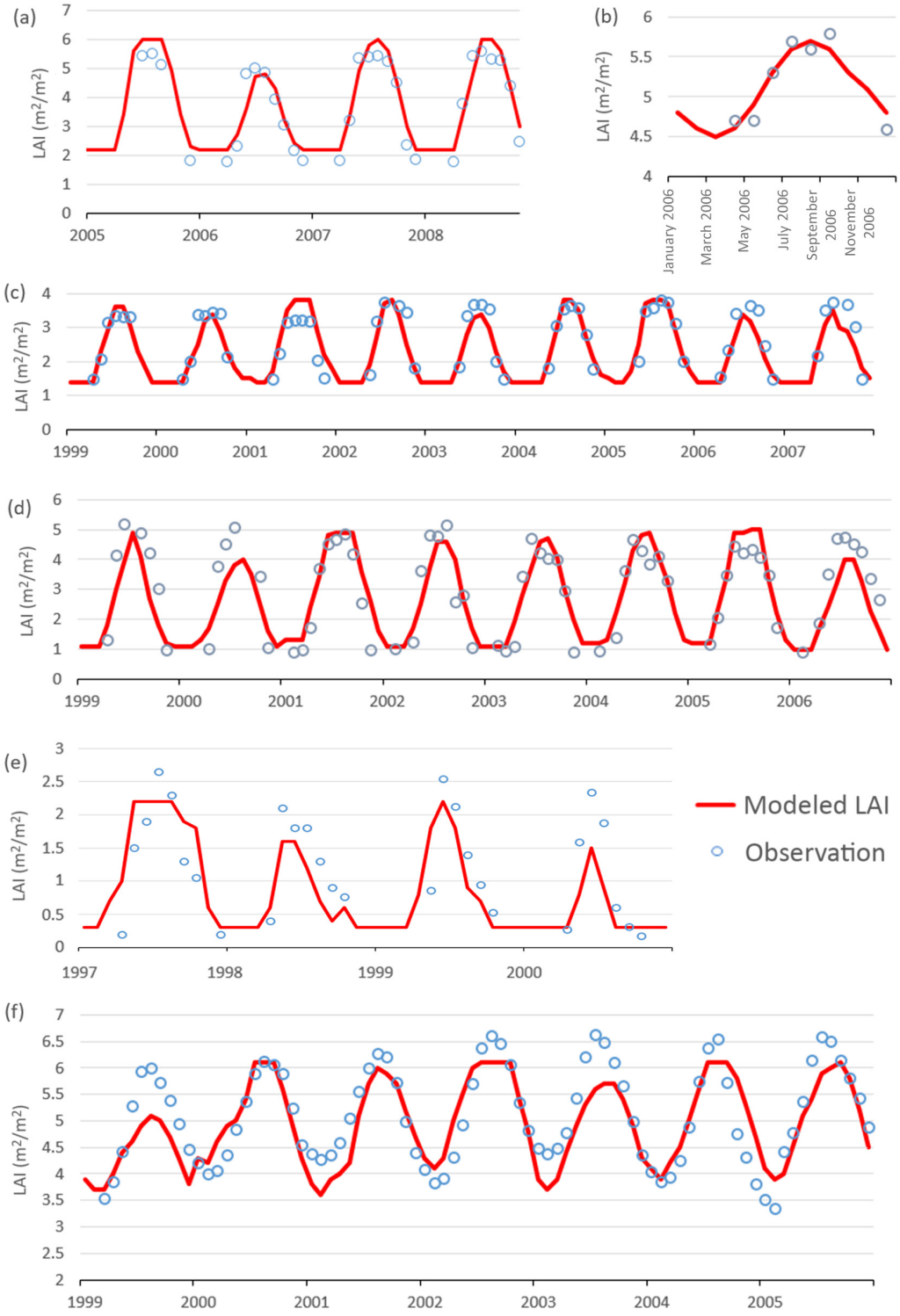

Fig. 2. Terrestrial ecosystem model-simulated LAI (m^2/m^2) by applying the optimal parameters and in situ observational data, data assimilation is conducted for sites (a) Harvard Forest, (b) Howland forest, (c) University of Michigan Biological Station, (d) Morgan Monroe State Forest, (e) Shidler Tallgrass Prairie and (f) Donaldson. LAI, leaf area index.

Table 1. Description of AmeriFlux sites with observed LAI for site-level data assimilation.

Site name/FLUXNET ID	Longitude (degree)	Latitude (degree)	Plant function type	Data period	Reference
Harvard Forest/US-Ha1	−72.17	42.54	Deciduous broadleaf forest	2005–2008	van Gorsel et al. (2009)
UMBS/US-UMB	−84.71	45.56	Deciduous broadleaf forest	1999–2007	
Howland Forest/US-Ho1	−68.74	45.2	Evergreen needleleaf forest	2006	Hagen et al. (2006)
Morgan Monroe State Forest/US-MMS	−86.41	39.32	Deciduous broadleaf forest	1999–2006	Richardson et al. (2012)
Shidler Tallgrass Prairie/US-Shd	−96.68	36.93	Grasslands	1997–2000	Schwalm et al. (2010)
Donaldson/US-SP3	−82.16	29.75	Evergreen needleleaf forest	1999–2007	Bracho et al. (2012)

Note: LAI, leaf area index; UMBS, University of Michigan Biological Station.

calculated as the function of maximum rate of photosynthesis carbon, atmospheric CO_2 concentration, leaf phenology, temperature, light use, and other factors (Zhuang et al. 2003). Leaf area index is estimated based on specific leaf area (*sla*):

$$\mathrm{LAI}(t) = sla \times l_A(t) \times leaf(t) \quad (2)$$

where *sla* is defined as the ratio of leaf area to dry leaf mass with units of $m^2 \cdot g^{-1} \cdot C^{-1}$, which is one of the widely accepted leaf characteristics to study leaf traits (Wilson et al. 1999). $l_A(t)$ (g C/m^2) is maximum biomass of the canopy, which is defined as a function of V_c:

$$l_A(t) = \frac{leafmxc}{1 + kleaf \times e^{\mathrm{cov} \times V_C}} \quad (3)$$

where *leaf*(*t*) is a scalar and is calculated as follows:

$$leaf(t) = \begin{cases} minleaf, \text{where} \frac{Uleaf_i(t)}{Uleaf_{i-1,\max}} < minleaf \\ \frac{Uleaf_i(t)}{Uleaf_{i-1,\max}}, \text{elsewhere} \\ 1, \quad \text{where} \frac{Uleaf_i(t)}{Uleaf_{i-1,\max}} > 1 \end{cases} \quad (4)$$

The value of *leaf*(*t*) resides between *minleaf* and 1, and the value in between is computed as the ratio of *Uleaf*(*t*) in each month to maximum *Uleaf*(*t*) of the previous year.

$Uleaf_i(t)$ represents the photosynthetic capacity of mature vegetation:

$$Uleaf_i(t) = aleaf \times \frac{\mathrm{EET}}{\mathrm{EET}_{\max}} + bleaf \times Uleaf_{i-1} + cleaf \quad (5)$$

where *aleaf*, *bleaf*, *cleaf*, and *minleaf* are coefficients for the calculation of $Uleaf_i(t)$. $Uleaf_i(t)$ is related to the estimated evapotranspiration (ET) and three parameters optimized using the data assimilation method. EET is the estimated ET, computed from a water balance model (Vörösmarty et al. 1998). $\mathrm{EET}_{\max}$ is the estimated maximum ET of previous year. Parameters related to LAI simulation also include *leafmxc*, *kleaf*, and *cov* (biome-specific foliage projection cover parameter). Different PFTs have different sets of optimal parameters.

Model parameterization

Site-level parameterization for LAI is conducted for different PFTs at the selected sites using observational data. At regional levels, an optimum set of parameters for each pixel is obtained using a spatially explicit parameterization method (Chen and Zhuang 2012). Specifically, we generate optimum parameters for each 0.5° × 0.5° grid using AVHRR LAI product from 1985 to 1995 while the data for the period of 1995–2010 are used for model evaluation at the regional scale.

To use in situ and satellite data of LAI to parameterize the model, a MCMC technique is used (Metropolis et al. 1953, Hastings 1970). Markov Chain Monte Carlo is a general method for simulation of stochastic processes with a specific probability density function. Specifically, a sequence of random variables is a Markov chain when the $(n + 1)$th element only depends on the nth element. One popular method to implement MCMC uses the metropolis-hasting algorithm. The basic idea of the algorithm is to generate random walk values with a proposed probability density and decide whether to accept or reject a value based on an acceptance ratio. Here, we sample 10,000 parameter combinations for each site with probability *P(x)*. The algorithm is with following steps:

Table 2. Prior values of parameters related to leaf area index estimation.

Acronym	Definition	Units	Mean	Standard deviation
leafmxc	Maximum biomass of the canopy	g C/m^2	500	250
kleafc	Biome-specific allocation parameter	None	2	1
sla	Specific leaf area	m^2/(gC)	0.008	0.004
cov	Biome-specific foliage projection cover parameter	None	−0.005	−0.0025
minleaf	Minimum photosynthesis capacity	None	0.5	0.25
aleaf	Coefficient A to model relative photosynthetic capacity of vegetation	None	0.5	0.25
bleaf	Coefficient B to model relative photosynthetic capacity of vegetation	None	0.5	0.25
cleaf	Coefficient C to model relative photosynthetic capacity of vegetation	None	0	0.5

1. Initialization: First, choose an arbitrary $\vec{x_0}$ as the initial sample, which is the initial vector of parameters space. In the case of LAI model, $\vec{x_0}$ represents $(leafmxc_0, kleafc_0, sla_0, \mathrm{cov}_0, minleaf_0, aleaf_0, bleaf_0, cleaf_0)$. Second, choose an arbitrary Gaussian distribution $Q(\vec{x_1}|\vec{x_0})$ (centered at $\vec{x_0}$) as the proposed density (or jumping distribution) for the sampling sequence (see Table 2 for details about initial parameter and distribution settings).
2. Iteration: For each time step t, generate candidate sample $\vec{x}_c$ based on $Q(\vec{x}_c|\vec{x}_t)$; then calculate an acceptance ratio $P(\vec{x}_c)/P(\vec{x}_t)$; if it is greater than or equals 1, accept the candidate and set $\vec{x}_{t+1} = \vec{x}_C$; if it is smaller than 1 and >0, accept the candidate with a probability of the acceptance ratio. If it is not >0, set $\vec{x}_{t+1} = \vec{x}_t$.

The Gaussian distribution $Q(\vec{x}_c|\vec{x}_t)$ is defined with a mean (the previous value for the parameter) and standard deviation (50% of the original value for the parameter) (Table 2). The best parameters for a pixel are optimized by calculating the root-mean-square error (RMSE) between model simulations and AVHRR LAI. Global land surface satellite LAI data are used for evaluating the model parameters by comparing with model simulations.

Regional simulations and analysis

For the regional analysis in North America, simulations are conducted for each grid with the optimized spatially explicit parameters for the region. The regional simulated data are organized to compute regional correlations between model and satellite product. We also examine the spatial distribution of parameter values. The sensitivity analysis is done by varying parameter values in the prior parameter distribution space. Furthermore, we separate the modeling results by sub-regions including Alaska, Canada, the conterminous United States and by PFTs to examine the decadal and seasonal LAI changes for different ecosystem types and areas in the region.

Results and Discussion

Comparison between modeled and observed leaf area index

Site-level data assimilations provide a set of optimum parameters for the six sites (Tables 1, 3). The parameters are evaluated with the reserved

Table 3. Best parameters for LAI modeling at calibration sites.

Site	Harvard Forest	UMBS	Howland Forest	Morgan Monroe State Forest	Shidler Tallgrass Prairie	Donaldson
leafmxc	653.586	579.135	634.889	702.178	585.261	590.308
kleafc	1.775	2.172	2.225	2.825	2.113	1.902
sla	0.0094	0.0066	0.0099	0.0071	0.0114	0.0103
cov	−0.000521	−0.001031	−0.000616	−0.000329	−0.00031	−0.0006
minleaf	0.367	0.375	0.542	0.194	0.128	0.49
aleaf	0.797	0.343	0.181	0.239	0.592	0.224
bleaf	0.527	0.487	0.674	0.463	0.434	0.649
cleaf	0.135	0.13	0.374	0.0195	−0.115	0.102

Note: LAI, leaf area index; UMBS, University of Michigan Biological Station.

Table 4. Model-data fitting statistics of site-level LAI between model simulations and observations.

Site	Correlation coefficient	Slope	Intercept (m^2/m^2)	RMSE (m^2/m^2)
Harvard Forest	0.96	0.93	0.50	0.49
UMBS	0.87	0.78	0.57	0.40
Howland Forest	0.96	0.82	0.97	0.15
Morgan Monroe State Forest	0.85	0.73	0.76	0.78
Shidler Tallgrass Prairie	0.82	0.67	0.33	0.49
Donaldson	0.75	0.59	2.06	0.67

Note: LAI, leaf area index; RMSE, root-mean-square error; UMBS, University of Michigan Biological Station.

data that have not been used for parameterization. For various ecosystems, the RMSE between observed and simulated LAI is smaller than 0.8 m^2/m^2 and correlation coefficients are >0.75 (Table 4, Fig. 2). The seasonality of the observed LAI is well produced with the model. The site-level simulations are also compared well with GLASS LAI product at different sites (RMSE ranging from 0.15 to 0.78 m^2/m^2).

Spatially explicit parameterization shows that the parameters are with different magnitudes for each PFT (Table 5, Fig. 3). Some parameters such as *kleafc* and *sla* have smaller spatial variations compared to other parameters such as *aleaf* and *bleaf*. This is because some parameters are more directly related to LAI in the model. Our previous study demonstrated that the varying parameters across space better simulated ecosystem carbon dynamics (Chen and Zhuang 2012). We thus use the derived spatially explicit parameters based on satellite data for our regional LAI simulation.

At the regional scale, the simulated LAI for each PFT varied across space, and the simulation compares well with the satellite data for each PFT (Table 6). The TEM performs well for all representative PFTs with R^2 ranging from 0.66 to 0.80 and RMSE from 1.05 to 2.32 m^2/m^2. For boreal forest as a major PFT in this region, the model performs well with R^2 of 0.76 and RMSE of 1.12 m^2/m^2. For other seven PFTs, the model performs similarly with RMSE <2.4 m^2/m^2.

The regression between simulated and remote sensing-based monthly LAI has the slope of 1.38 and 0.84, which is close to 1, for tundra and grasslands, respectively (Fig. 4). In addition, satellite-based LAI is saturated at 6 m^2/m^2, while TEM-modeled LAI has more reasonable values. In general, the model performs well for tundra, boreal forest, temperate coniferous/deciduous forest, grasslands, and xeric shrublands and slightly deteriorates for temperate deciduous forests (RMSE = 2.32 m^2/m^2) (Table 6). Using the spatially explicit parameters, the TEM better simulates LAI compared to using a single set of parameters for each PFT in the region. The correlation analysis suggests that monthly LAI is highly correlated with temperature (R^2 = 0.76) and precipitation (R^2 = 0.46) in North America.

Table 5. Optimal parameters from regional assimilation organized by plant function type from 1985 to 2010.

Type	Leafmxc	kleafc	sla	cov	minleaf	aleaf	bleaf	cleaf
Alpine tundra and polar desert	642 ± 240	1.66 ± 0.16	0.010 ± 0.003	−0.0006 ± 0.0045	0.11 ± 0.17	0.60 ± 0.15	0.39 ± 0.07	0.10 ± 0.04
Wet tundra	442 ± 235	1.67 ± 0.14	0.008 ± 0.002	−0.0004 ± 0.0011	0.22 ± 0.19	0.53 ± 0.17	0.38 ± 0.07	0.11 ± 0.06
Boreal forest	578 ± 203	1.68 ± 0.42	0.008 ± 0.001	−0.0013 ± 0.0097	0.08 ± 0.13	0.50 ± 0.13	0.37 ± 0.05	0.12 ± 0.02
Temperate coniferous forest	714 ± 154	1.76 ± 0.82	0.009 ± 0.002	−0.0115 ± 0.0315	0.27 ± 0.22	0.38 ± 0.15	0.38 ± 0.11	0.12 ± 0.06
Temperate deciduous forest	649 ± 155	1.66 ± 0.89	0.008 ± 0.001	−0.0373 ± 0.0482	0.12 ± 0.18	0.52 ± 0.19	0.35 ± 0.09	0.11 ± 0.04
Grassland	575 ± 208	1.66 ± 0.13	0.010 ± 0.003	−0.0003 ± 0.0000	0.23 ± 0.21	0.50 ± 0.20	0.37 ± 0.11	0.11 ± 0.05
Xeric shrubland	399 ± 227	1.67 ± 0.13	0.008 ± 0.001	−0.0003 ± 0.0002	0.40 ± 0.18	0.43 ± 0.19	0.40 ± 0.15	0.13 ± 0.08
Tropical forest	615 ± 197	2.09 ± 1.18	0.008 ± 0.001	−0.0332 ± 0.0468	0.45 ± 0.15	0.34 ± 0.21	0.48 ± 0.18	0.09 ± 0.14

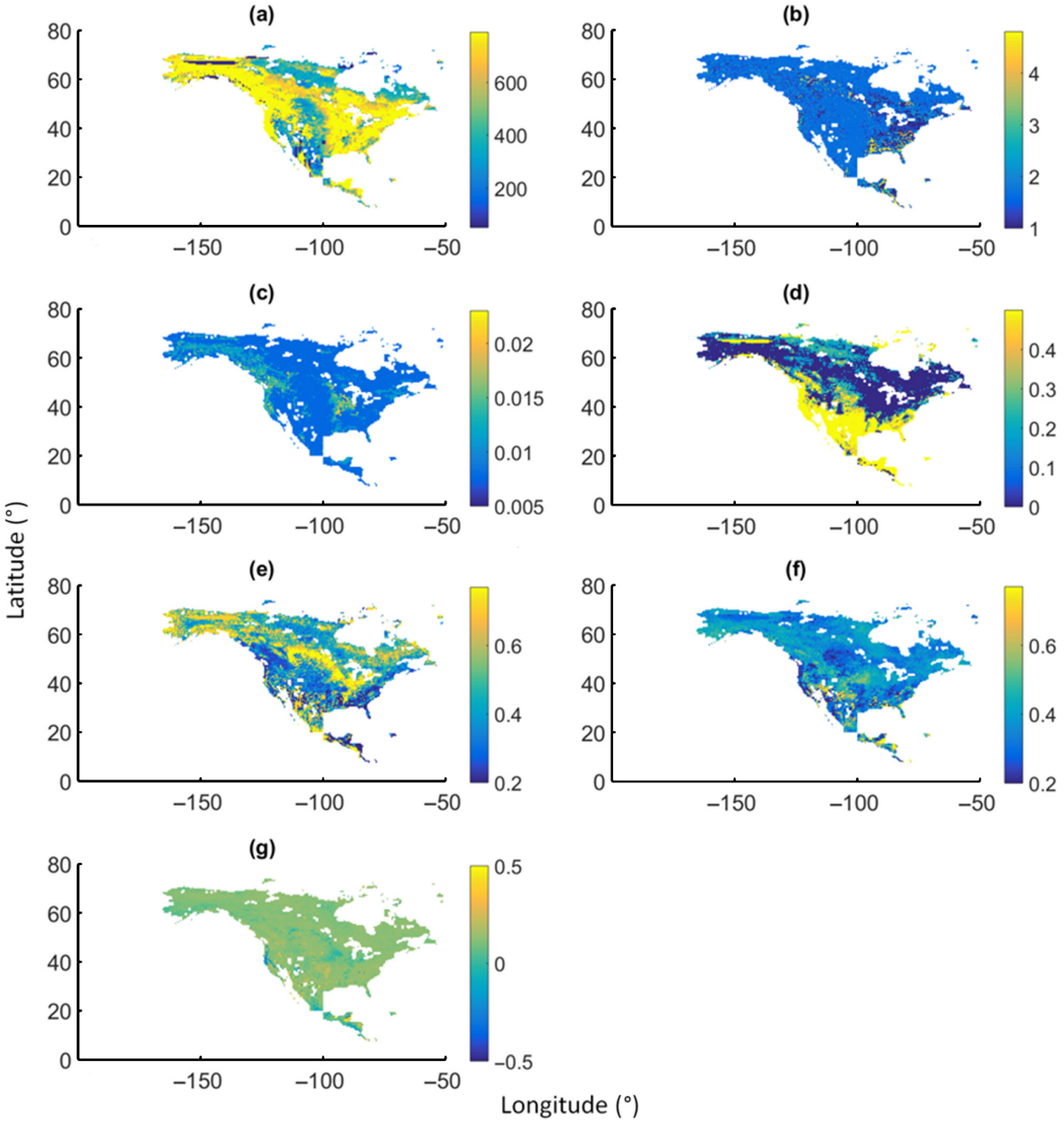

Fig. 3. Distribution of optimum parameters for spatially explicit regional simulations: (a) leafmxc (gC/m^2), (b) kleaf, (c) sla ($m^2/(gc)$), (d) minleaf (unitless), (e) aleaf (unitless), (f) bleaf (unitless), (g) cleaf (unitless).

Temperature plays a more significant role in LAI changes (Table 7).

To determine the distribution of LAI changes in North America, three sub-regions including Alaska, Canada, and the conterminous United States are analyzed (Fig. 5). In Alaska, monthly LAI did not change significantly with an increase of 0.02 m^2/m^2 from 2001 to 2010 compared with that in 1981–1990. The highest monthly average is in September, from 1.68 to 1.86 m^2/m^2. In Canada, monthly average LAI increased by 0.015 m^2/m^2 and RMSE < 0.1 m^2/m^2. In the conterminous United States, there was the largest increase by 0.06 m^2/m^2, with an ineligible

Table 6. Fitting statistics of regional leaf area index simulations and satellite data.

Plant function type	Number of simulation grids	R^2	RMSE (m^2/m^2)
Alpine tundra and polar desert	510	0.71	2.25
Wet tundra	1432	0.76	1.05
Boreal forest	3613	0.76	1.12
Temperate coniferous forests	1496	0.66	1.15
Temperate deciduous forests	449	0.67	1.32
Grasslands	1541	0.76	1.35
Xeric shrublands	725	0.69	1.27
Tropical forests	345	0.80	2.13

RMSE, root-mean-square error.

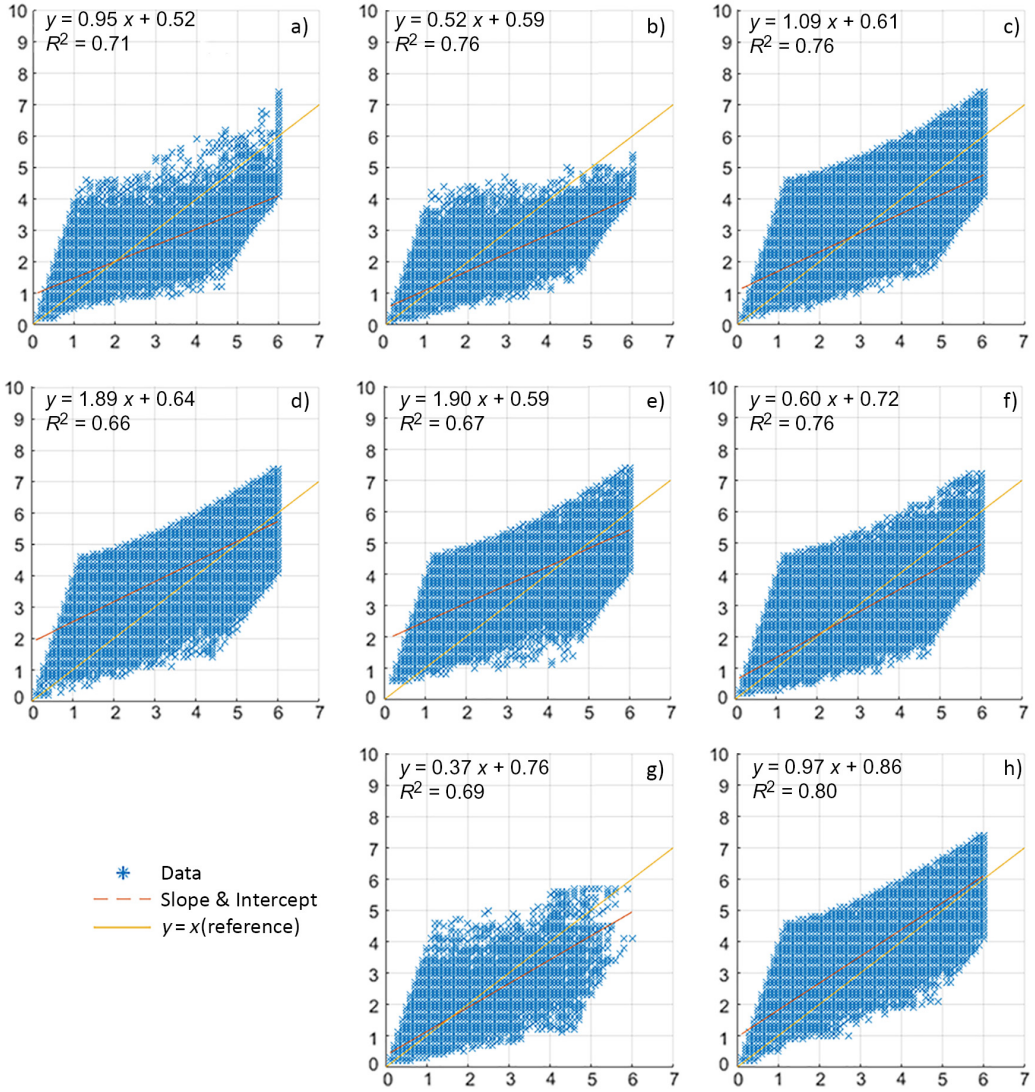

Fig. 4. Comparison between simulated monthly leaf area index (LAI) (m^2/m^2) and remote-sensing (advanced very high-resolution radiometer) LAI product of North America categorized by plant function type: (A) Alpine tundra and polar desert; (B) Wet Tundra; (C) Boreal forest; (D) Temperate coniferous forests; (E) Temperate deciduous forests; (F) Grasslands; (G) Xeric Shrublands; (H) Xeric Woodland. *Y*-axis is simulated data, and *X*-axis is satellite data.

Table 7. Correlation between forcing data and modeled LAI.

Site	(a)	(b)
Harvard Forest	0.75	0.48
UMBS	0.72	0.52
Howland Forest	0.65	0.42
Morgan Monroe State Forest	0.68	0.45
Shidler Tallgrass Prairie	0.52	0.39
Donaldson	0.55	0.41

Notes: LAI, leaf area index; UMBS, University of Michigan Biological Station. Column (a) shows correlation between LAI and temperature; column (b) shows correlation between LAI and precipitation.

increase (>0.1 m^2/m^2) from September to December. The conterminous United States contributes the most to the average LAI increase in North America during the three-decade study period. The modeled LAI fits best with satellite-based LAI product in the conterminous United States (R^2 = 0.81, slope = 0.78), while model also captures the satellite-based LAI for Alaska and Canada (Fig. 5).

Different sub-regions show various correlations with climate. In Canada, monthly LAI has higher correlations (R^2 = 0.78) with air temperature than in the conterminous United States (R^2 = 0.68), while lower correlations with precipitation (R^2 = 0.30) than in the conterminous United States (R^2 = 0.58). Leaf phenology in higher latitude regions are more affected by temperature and less by precipitation (Table 8).

From 1985 to 2010, temperate coniferous and temperate deciduous LAI increased by 0.03 and 0.06 m^2/m^2, respectively. The increase of monthly LAI of deciduous forests is mostly due to increased monthly mean temperature. Overall, TEM captures the maximum and minimum monthly LAI for wet tundra, boreal forests, temperate coniferous forests, temperate deciduous forests, grasslands, and xeric shrublands, with RMSE < 0.5 m^2/m^2. Average monthly LAI shows different trends for different PFTs (Fig. 4). We further separated the conterminous United States into four sub-regions including southwest (California, Nevada, Utah, Colorado, Arizona, New Mexico, Oklahoma, and Texas), southeast (Arkansas, Louisiana, Mississippi, Alabama, Georgia, Florida, South Carolina, Tennessee, North Carolina, Kentucky, Virginia, and West Virginia), northwest (Washington, Oregon, Idaho, Montana, Wyoming), and northeast (Maine, New Hampshire, Vermont, Massachusetts, Rhode Island, Connecticut, New York, New Jersey, and Pennsylvania). TEM performs similarly for these sub-regions with R^2 ranging from 0.65 to 0.86. In the northwest, the model performs the best (R^2 = 0.86) (Fig. 6).

Phenology change analysis

Our modeled LAI results indicate that there was a phenology trend of earlier spring and later autumn, which have been reported in several previous studies (Myneni et al. 1997*a, b*, Barichivich et al. 2013, Keenan et al. 2014). Modeled monthly LAI in April and September all increased between two decades from 1981–1990 to 2001–2010 at 0.03 m^2/m^2 for April and 0.24 m^2/m^2 for September, respectively (Fig. 7). There was an increase of LAI at 0.3 m^2/m^2 between the 1980s and 2000s in majority area of North America. The exception occurs mostly at high latitudes or lands covered with vegetation that typically has low LAI. Similarly, AVHRR LAI data product also indicated that there was an increase of monthly LAI in April and September from the 1980s to 1990s, especially in the conterminous United States, demonstrating phenology changed with an earlier leaf start and later leaf fall. Analysis for each PFT shows temperate deciduous forests had the most obvious change. Our temporal regression between LAI in April and September and time shows positive correlations for April (R^2 = 0.72) and September (R^2 = 0.64), respectively, suggesting there are significant increases of April and September LAI over the period.

In general, the region had an earlier greening trend from March to June, primarily due to temperature increasing during the study period (Fig. 5). April LAI increased more in the conterminous United States (0.04 m^2/m^2) compared to Alaska (0.003 m^2/m^2) and Canada (0.001 m^2/m^2). Similarly, the increase of LAI also occurred in September in

Table 8. Correlation between forcing data and LAI simulation for each sub-region.

Sub-region in North America	(a)	(b)
Alaska	0.56	0.43
Canada	0.78	0.3
Conterminous United States	0.68	0.58

Notes: LAI, leaf area index. Column (a) shows correlation between LAI and temperature; column (b) shows correlation between LAI and precipitation.

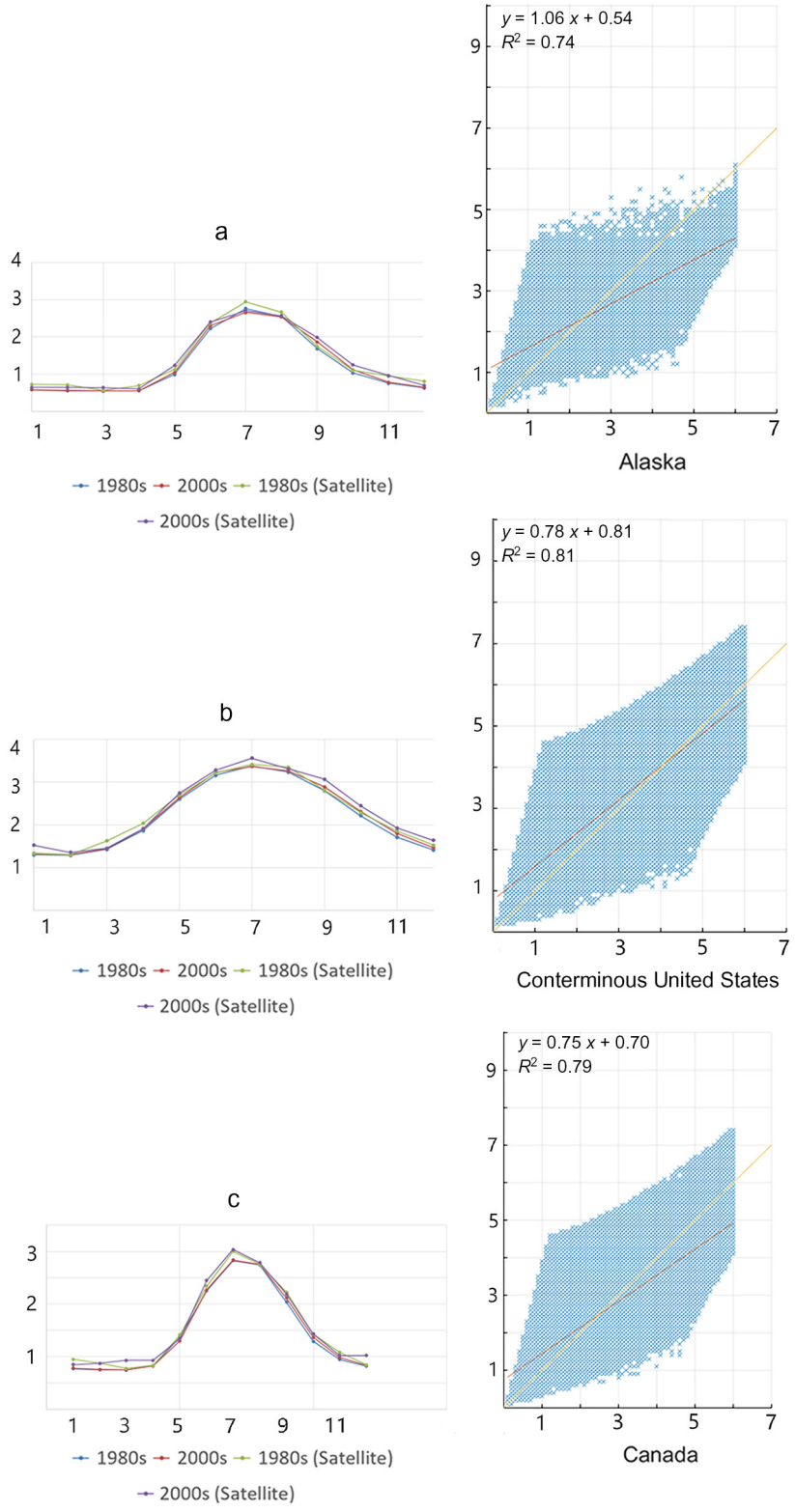

Fig. 5. Comparison between modeled and satellite-based monthly average leaf area index for three

(Fig. 5. *Continued*)
sub-regions in North America: (a) Alaska; (b) Conterminous United States; (c) Canada. *Y*-axis is simulated data, and *X*-axis is satellite data.

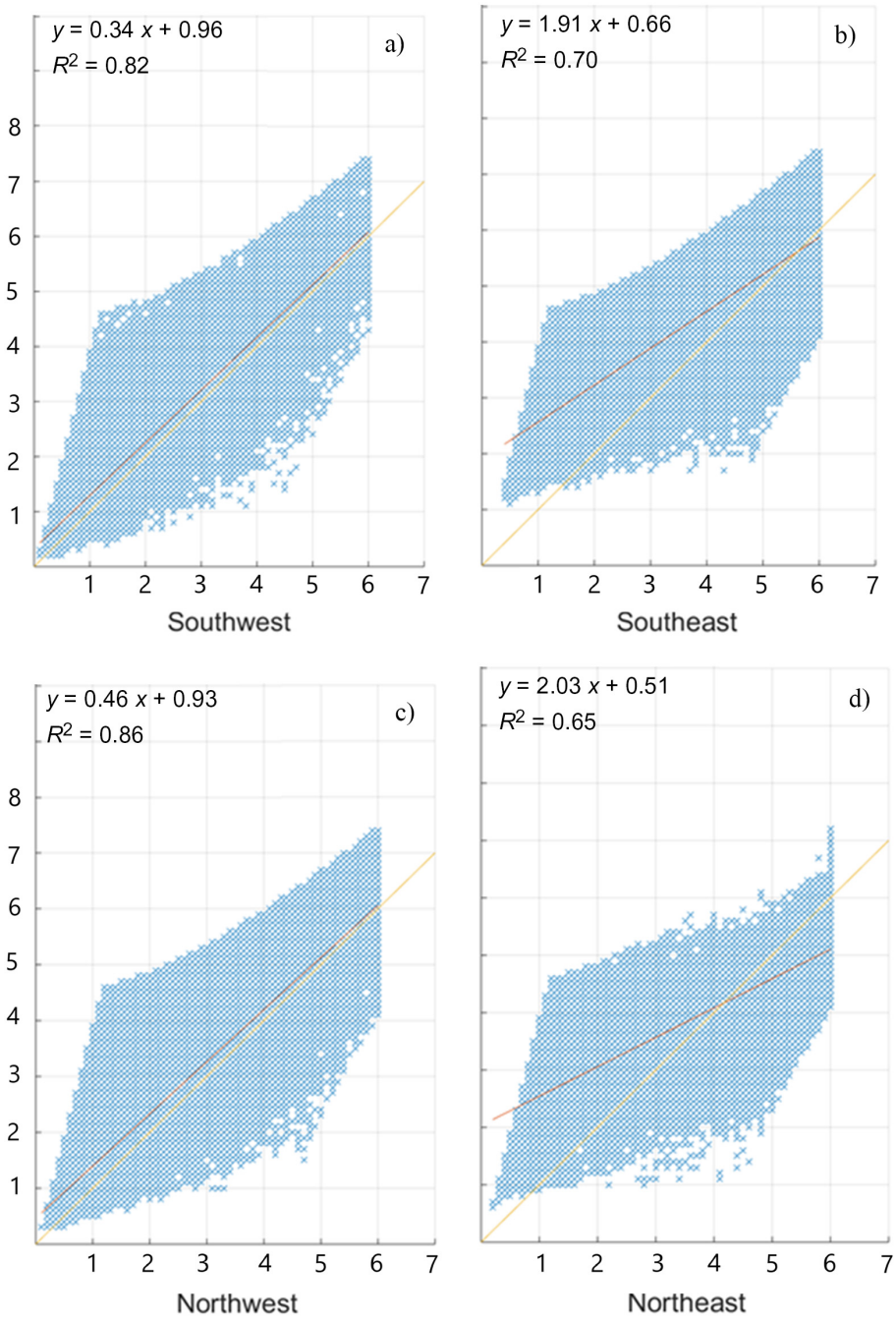

Fig. 6. Comparison between modeled (*Y*-axis) and satellite-based (*X*-axis) monthly average leaf area index for four sub-regions in the Conterminous United States: (a) Southwest; (b) Southeast; (c) Northwest, (d) Northeast.

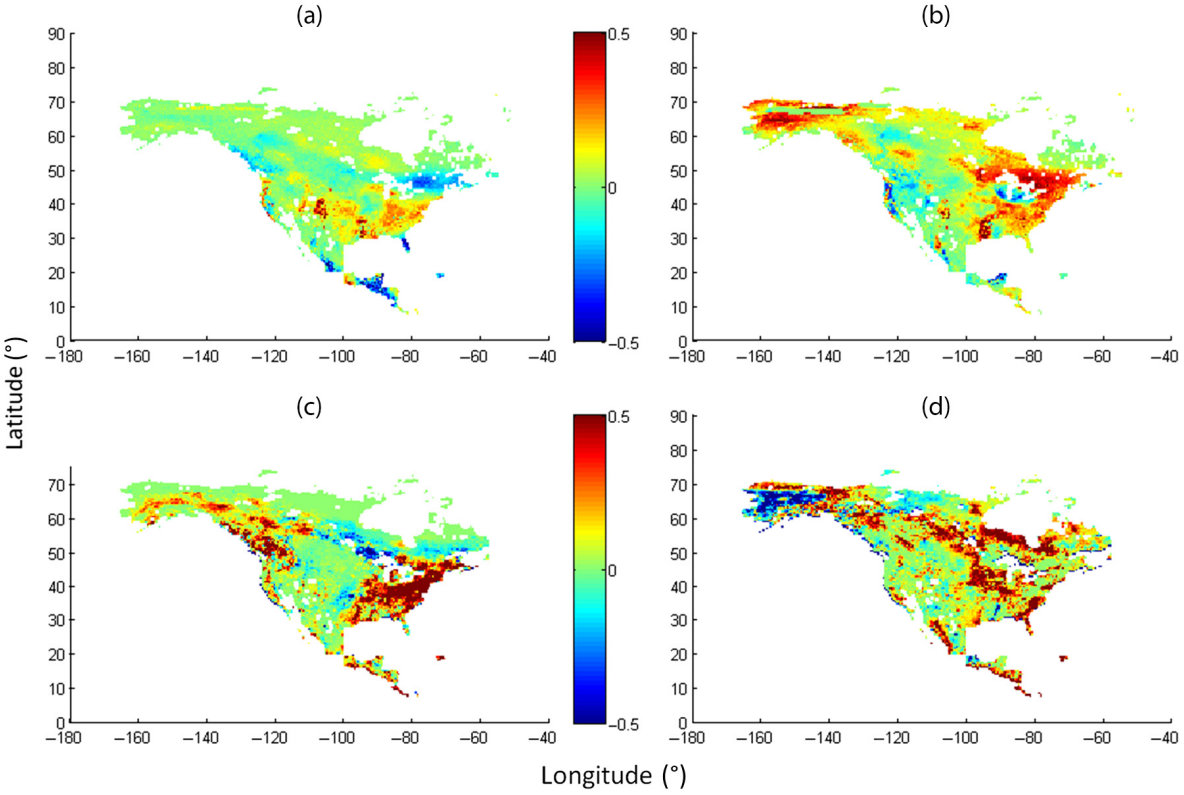

Fig. 7. Average monthly terrestrial ecosystem model-modeled leaf area index (LAI) increase in April (a) and September (b) from 1981–1990 to 2001–2010; Average monthly advanced very high-resolution radiometer LAI increase in April (c) and September (d) from 1985–1990 to 1991–2000.

Alaska (0.05 m^2/m^2), Canada (0.04 m^2/m^2), and the conterminous United States (0.27 m^2/m^2).

Compared with other recent studies focused on phenology in North America using remote-sensing data (Richardson et al. 2012, Melaas et al. 2016), our simulations showed similar patterns of earlier spring onset and longer growing season in the region. However, the shift of the end of growing season is harder to capture than the start of growing season in our simulations.

Greening feature characterized as increasing LAI varied among different PFTs (Fig. 7). Temperate deciduous forests had a larger increase than other PFTs, with 0.07 m^2/m^2 in April and 0.31 m^2/m^2 in September. Boreal forests, accounting for 30% grids in North America, had an increase of 0.04 m^2/m^2 in April and 0.27 m^2/m^2 in September, respectively. Previous studies have demonstrated the response of vegetation phenology to warming climate in a similar way (e.g., Zhang et al. 2007). In addition to the increased LAI magnitude, it is widely acknowledged that the timing of phenological events including start and end of growing season is sensitive to climate change in various regions (Chuine et al. 2004, Liu et al. 2016). Our analysis indicates that the timing of the leaf start and leaf fall is significantly and positively correlated ($R^2 > 0.5$, P-value < 0.01) between modeled LAI in April and September (Fig. 8), suggesting that the growing season length has increased in the last few decades in North America, which is consistent with recent studies (Myneni et al. 1997*a*, *b*, Keenan et al. 2014).

Our LAI and phenology analysis is limited by the availability of quality observation data of LAI. Leaf area index data are often only available for growing season at observational sites. Thus, the parameters are not well constrained for capturing the LAI seasonality. Our uncertainty analysis by varying parameters of LAI within the prior probability distribution indicates that the simulated monthly regional LAI varies by 36% (Fig. 9). For

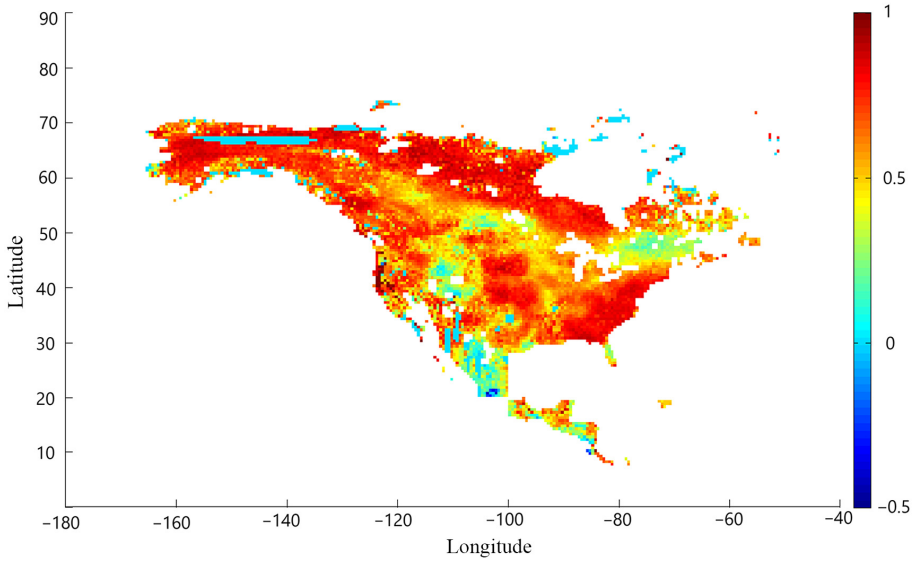

Fig. 8. Correlation coefficients between terrestrial ecosystem model-simulated leaf area index in April and September from 1985 to 2010.

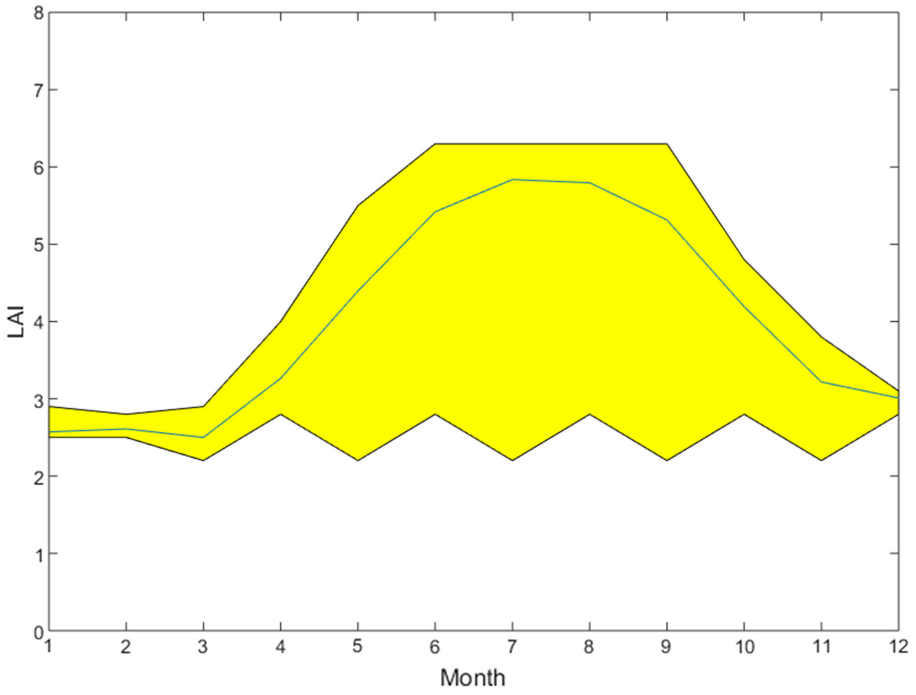

Fig. 9. Uncertainty analysis of modeled regional leaf area index (LAI) by varying parameters between 1985 and 2010: upper bound, lower bound, and mean month LAI values.

the study period, the increase of regional LAI is (3 ± 0.5)% due to uncertain parameters. In addition, LAI is modeled as a function of vegetation carbon with a few parameters, which does not sufficiently represent the processes determining LAI. Future improvement shall include more biological processes related to leaf phenology.

Future applications of LAI modeling

Our next steps include integrating the improved LAI modeling into GPP and ET quantification with TEM. In previous studies of carbon dynamics with TEM (e.g., Zhu and Zhuang 2013), LAI was not used for modeling GPP. With our spatial-explicitly calibrated LAI, we now could improve GPP simulations, thus net primary production (NPP) and net ecosystem production defined as the difference of NPP and heterotrophic respiration. We will also be able to integrate LAI into ET quantification with TEM. Previously, we have used the Penman-Monteith equation to estimate ET by using satellite-based or observed LAI with TEM (e.g., Liu et al. 2013). With improved LAI modeling, we could improve the quantification of ET using TEM for certain time periods and spatial areas of interest that are not limited within satellite-based LAI periods and regions, such as for the 21st century and the whole North America. The improved LAI modeling within TEMs could also be an important component in earth system models to quantify feedbacks between terrestrial biosphere and the climate.

Conclusions

This study improves LAI algorithms within a process-based biogeochemistry model to study phenology patterns in North America. Observational LAI data from AmeriFlux network are used to optimize parameters. Remote-sensing data of AVHRR LAI product are used to optimize parameters at regional scales. Comparison between model simulations and satellite-based LAI for the region shows that the model is able to estimate the seasonality and interannual variability of LAI in the region. The average LAI in recent three decades has increased by 3% on average in the region. The simulated monthly average LAI increase during study period was 1.24, 1.46, and 2.21 m^2/m^2, in Alaska, Canada, and the conterminous United States, respectively, which is consistent with satellite observations. In comparison with satellite data, the model captured the phenology change for key plant functional types from 1985 to 2010. The model also performed well to capture the regional phenology change in Alaska, Canada, and the conterminous United States. This study provides a way to estimate the changes in LAI and phenology, which will improve future carbon and water cycling quantification for the region.

Acknowledgments

This research was supported by a NSF project (no. 1028291) funded to Q.Z. We acknowledge the computing support from the Rosen Center for Advanced Computing at Purdue. We also acknowledge that the AmeriFlux network provides multiple LAI and other auxiliary datasets for this model-data fusion study.

Literature Cited

Anav, A., G. Murray-Tortarolo, P. Friedlingstein, S. Sitch, S. Piao, and Z. Zhu. 2013. Evaluation of land surface models in reproducing satellite Derived leaf area index over the high-latitude northern hemisphere. Part II: Earth system models. Remote Sensing 5:3637–3661.

Arora, V. K., and G. J. Boer. 2005. A parameterization of leaf phenology for the terrestrial ecosystem component of climate models. Global Change Biology 11:39–59.

Asner, G. P., J. M. Scurlock, and J. A. Hicke. 2003. Global synthesis of leaf area index observations: implications for ecological and remote sensing studies. Global Ecology and Biogeography 12: 191–205.

Asrar, G., M. Fuchs, E. T. Kanemasu, and J. L. Hatfield. 1984. Estimating absorbed photosynthetic radiation and leaf area index from spectral reflectance in wheat. Agronomy Journal 76:300–306.

Asrar, G., R. B. Myneni, Y. Li, and E. T. Kanemasu. 1989. Measuring and modeling spectral characteristics of a tallgrass prairie. Remote Sensing of Environment 27:143–155.

Balzarolo, M., et al. 2016. Matching the phenology of net ecosystem exchange and vegetation indices estimated with MODIS and FLUXNET in-situ observations. Remote Sensing of Environment 174: 290–300.

Baret, F., and G. Guyot. 1991. Potentials and limits of vegetation indices for LAI and APAR assessment. Remote Sensing of Environment 35:161–173.

Barichivich, J., et al. 2013. Large-scale variations in the vegetation growing season and annual cycle of atmospheric CO2 at high northern latitudes from 1950 to 2011. Global Change Biology 19:3167–3183.

Beaubien, E. G., and H. J. Freeland. 2000. Spring phenology trends in Alberta, Canada: links to ocean temperature. International Journal of Biometeorology 44:53–59.

Beck, P. S., C. Atzberger, K. A. Høgda, B. Johansen, and A. K. Skidmore. 2006. Improved monitoring of vegetation dynamics at very high latitudes: A new method using MODIS NDVI. Remote Sensing of Environment 100:321–334.

Bracho, R., G. Starr, H. L. Gholz, T. A. Martin, W. P. Cropper, and H. W. Loescher. 2012. Controls on carbon dynamics by ecosystem structure and climate for southeastern U.S. slash pine plantations. Ecological Monographs 82:101–128.

Chen, J. M., and T. A. Black. 1992. Defining leaf area index for non-flat leaves. Plant, Cell and Environment 15:421–429.

Chen, J. M., and J. Cihlar. 1996. Retrieving leaf area index of boreal conifer forests using Landsat TM images. Remote Sensing of Environment 55: 153–162.

Chen, M., and Q. Zhuang. 2012. Spatially explicit parameterization of a terrestrial ecosystem model and its application to the quantification of carbon dynamics of forest ecosystems in the conterminous United States. Earth Interactions 16:1–22.

Chmielewski, F. M., and T. Rötzer. 2001. Response of tree phenology to climate change across Europe. Agricultural and Forest Meteorology 108:101–112.

Chuine, I., P. Yiou, N. Viovy, B. Seguin, V. Daux, and E. L. R. Ladurie. 2004. Historical phenology: grape ripening as a past climate indicator. Nature 432: 289–290.

Claverie, M., J. L. Matthews, E. F. Vermote, and C. O. Justice. 2016. A 30+ year AVHRR LAI and FAPAR climate data record: Algorithm description and validation. Remote Sensing 8:263.

Felzer, B., D. Kicklighter, J. Melillo, C. Wang, Q. Zhuang, and R. Prinn. 2004. Effects of ozone on net primary production and carbon sequestration in the conterminous United States using a biogeochemistry model. Tellus Series B 56:230–248.

Fisher, J. I., J. F. Mustard, and M. A. Vadeboncoeur. 2006. Green leaf phenology at Landsat resolution: Scaling from the field to the satellite. Remote Sensing of Environment 100:265–279.

Hagen, S. C., B. H. Braswell, E. Linder, S. Frolking, A. D. Richardson, and D. Y. Hollinger. 2006. Statistical uncertainty of eddy flux-based estimates of gross ecosystem carbon exchange at Howland Forest, Maine. Journal of Geophysical Research: Atmospheres 111. https://doi.org/10.1029/2005JD006154

Hastings, W. K. 1970. Monte Carlo sampling methods using Markov chains and their applications. Biometrika 57:97–109.

Hurley, M. A., M. Hebblewhite, J. M. Gaillard, S. Dray, K. A. Taylor, W. K. Smith, P. Zager, and C. Bonenfant. 2014. Functional analysis of Normalized Difference Vegetation Index curves reveals overwinter mule deer survival is driven by both spring and autumn phenology. Philosophical Transactions of the Royal Society B 369:20130196.

Jin, H., and L. Eklundh. 2014. A physically based vegetation index for improved monitoring of plant phenology. Remote Sensing of Environment 152: 512–525.

Keenan, T. F., et al. 2014. Net carbon uptake has increased through warming-induced changes in temperate forest phenology. Nature Climate Change 4:598–604.

Liang, S., et al. 2013. A long-term Global LAnd Surface Satellite (GLASS) data-set for environmental studies. International Journal of Digital Earth 6(Suppl 1):5–33.

Liang, L., et al. 2014. A cross comparison of spatiotemporally enhanced springtime phenological measurements from satellites and ground in a northern US mixed forest. IEEE Transactions on Geoscience and Remote Sensing 52:7513–7526.

Linkosalo, T., H. K. Lappalainen, and P. Hari. 2008. A comparison of phenological models of leaf bud burst and flowering of boreal trees using independent observations. Tree Physiology 28:1873–1882.

Liu, S., M. Chen, and Q. Zhuang. 2016. Direct radiative effects of tropospheric aerosols on changes of global surface soil moisture. Climatic Change 136: 175–187.

Liu, Y., Q. Zhuang, M. Chen, Z. Pan, N. Tchebakova, A. Sokolov, and Y. He. 2013. Response of evapotranspiration and water availability to changing climate and land cover on the Mongolian Plateau during the 21st century. Global and Planetary Change 108:85–99.

McGuire, A. D., J. M. Melillo, L. A. Joyce, D. W. Kicklighter, A. L. Grace, B. I. I. I. Moore, and C. J. Vorosmarty. 1992. Interactions between carbon and nitrogen dynamics in estimating net primary productivity for potential vegetation in North America. Global Biogeochemical Cycles 6: 101–124.

Melaas, E. K., D. Sulla-Menashe, J. M. Gray, T. A. Black, T. H. Morin, A. D. Richardson, and M. A. Friedl. 2016. Multisite analysis of land surface phenology in North American temperate and boreal

deciduous forests from Landsat. Remote Sensing of Environment 186:452–464.

Melillo, J. M., A. D. McGuire, D. W. Kicklighter, B. Moore, C. J. Vorosmarty, and A. L. Schloss. 1993. Global climate change and terrestrial net primary production. Nature 363:234–240.

Menzel, A., and P. Fabian. 1999. Growing season extended in Europe. Nature 397:659.

Metropolis, N., A. W. Rosenbluth, M. N. Rosenbluth, A. H. Teller, and E. Teller. 1953. Equation of state calculations by fast computing machines. Journal of Chemical Physics 21:1087–1092.

Myneni, R. B., C. D. Keeling, C. J. Tucker, G. Asrar, and R. R. Nemani. 1997*a*. Increased plant growth in the northern high latitudes from 1981-1991. Nature 386:698–701.

Myneni, R. B., R. R. Nemani, and S. W. Running. 1997*b*. Algorithm for the estimation of global land cover, LAI and FPAR based on radiative transfer models. IEEE Transactions on Geoscience and Remote Sensing 35:1380–1393.

Raich, J. W., et al. 1991. Potential net primary productivity in South America: application of a global model. Ecological Applications 1:399–429.

Richardson, A. D., et al. 2012. Terrestrial biosphere models need better representation of vegetation phenology: results from the North American Carbon Program Site Synthesis. Global Change Biology 18:566–584.

Schwalm, C. R., et al. 2010. A model-data intercomparison of CO_2 exchange across North America: results from the North American Carbon Program site synthesis. Journal of Geophysical Research: Biogeosciences 115. https://doi.org/10.1029/2009JG001229

Sulman, B. N., A. R. Desai, B. D. Cook, N. Saliendra, and D. S. Mackay. 2009. Contrasting carbon dioxide fluxes between a drying shrub wetland in Northern Wisconsin, USA, and nearby forests. Biogeosciences 6(6):1115–1126.

Sung, S., and R. M. Amasino. 2004. Vernalization in Arabidopsis thaliana is mediated by the PHD finger protein VIN3. Nature 427:159–164.

Urbanski, S., C. Barford, S. Wofsy, C. Kucharik, E. Pyle, J. Budney, K. McKain, D. Fitzjarrald, M. Czikowsky, and J. W. Munger. 2007. Factors controlling CO2 exchange on timescales from hourly to decadal at Harvard Forest. Journal of Geophysical Research: Biogeosciences 112:G02020. https://doi.org/10.1029/2006JG000293

Van Gorsel, E., et al. 2009. Estimating nocturnal ecosystem respiration from the vertical turbulent flux and change in storage of CO_2. Agricultural and Forest Meteorology 149:1919–1930.

Vörösmarty, C. J., C. A. Federer, and A. L. Schloss. 1998. Potential evaporation functions compared on US watersheds: Possible implications for global-scale water balance and terrestrial ecosystem modeling. Journal of Hydrology 207:147–169.

Wilson, P. J., K. E. N. Thompson, and J. G. Hodgson. 1999. Specific leaf area and leaf dry matter content as alternative predictors of plant strategies. New Phytologist 143:155–162.

Yue, X., N. Unger, X. Zhang, and C. S. Vogel. 2015. Probing the past 30-year phenology trend of US deciduous forests. Biogeosciences 12:4693–4709.

Zhang, X., M. A. Friedl, C. B. Schaaf, A. H. Strahler, J. C. Hodges, F. Gao, B. C. Reed, and A. Huete. 2003. Monitoring vegetation phenology using MODIS. Remote Sensing of Environment 84:471–475.

Zhang, X., D. Tarpley, and J. T. Sullivan. 2007. Diverse responses of vegetation phenology to a warming climate. Geophysical Research Letters 34:L19405. https://doi.org/10.1029/2007GL031447

Zhu, Q., and Q. Zhuang. 2013. Improving the quantification of terrestrial ecosystem carbon dynamics over the United States using an adjoint method. Ecosphere 4:1–21.

Zhuang, Q., J. He, Y. Lu, L. Ji, J. Xiao, and T. Luo. 2010. Carbon dynamics of terrestrial ecosystems on the Tibetan Plateau during the 20th century: an analysis with a process-based biogeochemical model. Global Ecology and Biogeography 19:649–662.

Zhuang, Q., A. D. McGuire, K. P. O'neill, J. W. Harden, V. E. Romanovsky, and J. Yarie. 2002. Modeling soil thermal and carbon dynamics of a fire chronosequence in interior Alaska. Journal of Geophysical Research: Atmospheres 107: https://doi.org/10.1029/2001JD001244

Zhuang, Q., V. E. Romanovsky, and A. D. McGuire. 2001. Incorporation of a permafrost model into a large-scale ecosystem model: Evaluation of temporal and spatial scaling issues in simulating soil thermal dynamics. Journal of Geophysical Research: Atmospheres 106:33649–33670.

Zhuang, Q., et al. 2003. Carbon cycling in extratropical terrestrial ecosystems of the Northern Hemisphere during the 20th century: a modeling analysis of the influences of soil thermal dynamics. Tellus Series B 55:751–776.